nature chemistry

ARTICLES

https://doi.org/10.1038/s41557-018-0175-8

Chemoselective methylene oxidation in aromatic molecules

Jinpeng Zhao[1], Takeshi Nanjo[2], Emilio C. de Lucca Jr[3] and M. Christina White[1*]

Despite significant progress in the development of site-selective aliphatic C–H oxidations over the past decade, the ability to oxidize strong methylene C–H bonds in the presence of more oxidatively labile aromatic functionalities remains a major unsolved problem. Such chemoselective reactivity is highly desirable for enabling late-stage oxidative derivatizations of pharmaceuticals and medicinally important natural products that often contain such functionality. Here, we report a simple manganese small-molecule catalyst Mn(CF_3-PDP) system that achieves such chemoselectivity via an unexpected synergy of catalyst design and acid additive. Preparative remote methylene oxidation is obtained in 50 aromatic compounds housing medicinally relevant halogen, oxygen, heterocyclic and biaryl moieties. Late-stage methylene oxidation is demonstrated on four drug scaffolds, including the ethinylestradiol scaffold where other non-directed C–H oxidants that tolerate aromatic groups effect oxidation at only activated tertiary benzylic sites. Rapid generation of a known metabolite (piragliatin) from an advanced intermediate is demonstrated.

The majority of small-molecule therapeutics are comprised of functionalized hydrocarbon scaffolds containing a mixture of C(sp^2)–H bonds and increasingly more C(sp^3)–H bonds[1–4]. Reactions that effect the direct atomistic exchange of hydrogen with oxygen remote from such aromatic groups would avoid lengthy de novo synthesis for generating analogues and identifying metabolites; however, because of the challenges of hydroxylating an inert C–H bond in the presence of oxidatively more labile π-functionality, such transformations have not been fully realized in the laboratory. Iron enzymes are the only known catalysts capable of hydroxylation of strong aliphatic C–H bonds in the presence of π-functionality by means of restricted substrate access to the oxidant (Fig. 1a,b)[5], however, these enzymes are challenging to use on preparative scales (vide infra) and this supramolecular approach for achieving chemoselectivity has not been successful with small-molecule catalysts.

Despite recent advances in small-molecule catalysts for site-selective aliphatic C–H hydroxylations, none of these catalysts can effect strong aliphatic methylene C–H bond oxidation (bond dissociation energy (BDE) = 98 kcal mol^{-1}) in the presence of a range of aromatic groups[6–13]. Whereas C–H aminations, alkylations and halogenation reactions tolerate aromatic functionality[14–16], the only aromatic groups tolerated in higher-energy methylene C–H hydroxylations have been electronically deactivated with strong electron-withdrawing groups (that is, nitro, trifluoromethyl, triflate with > 0.5 *para*-Hammett sigma value (σ_p values))[10,11]. Ruthenium[6] and manganese[7,8] catalysts and stoichiometric oxidant methyl(trifluoromethyl)dioxirane (TFDO)[17] are tolerant of benzoate (σ_p = 0.45) and in a few cases phenyl functionality[6], but only in the hydroxylation of weaker benzylic C–H (BDE = 85 kcal mol^{-1}, Fig. 1c) or tertiary C(sp^3)–H bonds (BDE = 96 kcal mol^{-1}). The current state of the art suggests that to divert oxidation of labile aromatic functionalities, the catalyst's capacity for aliphatic hydroxylations must be reduced. We now demonstrate that, via the combination of Mn(CF_3-PDP) **1** catalyst (Fig. 1d) and chloroacetic acid additive, C(sp^3)–H oxidation can be achieved with an unprecedented combination of high chemoselectivity (that is, it tolerates medicinally important aromatic functionalities) and high reactivity (that is, it preparatively oxidizes aliphatic methylene C–H bonds) in the absence of directing groups or molecular recognition elements (Fig. 1c,d).

Results and discussion

Reaction development. We first investigated the oxidation of secondary methylene substrate **2** having a mildly electron-withdrawing bromo-substituted aryl moiety (σ_p = 0.23) with oxidants reported to be capable of oxidizing benzylic and tertiary C(sp^3)–H bonds in the presence of benzoates. Stoichiometric oxidant TFDO was evaluated under low-temperature conditions (reported to prevent free-radical formation[17]) as well as more forcing conditions[18]. Only the latter were effective at producing methylene oxidized product, albeit in poor yields and chemoselectivity (Table 1, entries 1–2). Ruthenium catalysts purported to be highly chemoselective for benzylic and tertiary C(sp^3)–H oxidations (Ru(Me_3TACN))[8] and *cis*-(Ru(dtbyp)$_2$$Cl_2$)[6] were not effective in oxidizing stronger methylene bonds (entries 3–4). Known manganese catalysts Mn(OTf)$_2$/bipyridine[8] and Mn(PDP)(OTf)$_2$[7] were evaluated under their previously reported conditions for C(sp^3)–H bond oxidation and found to furnish **3** in poor yields but encouraging chemoselectivities (entries 5–6).

The two primary mechanisms for aromatic oxidation with iron oxo enzymes (CYP450s) are single electron pathways at aromatic protein residues to generate radicals[19] and epoxidation of aromatic substrates followed by a rearrangement/hydride shift ('NIH shift')[20] to generate phenols (Fig. 1b)[5]. It is well-precedented that a switch from iron to manganese in catalysts that oxidize C–H bonds via high-valent metal heteroatom species (that is, metal oxos and nitrenes) leads to a reduction in their oxidation potential[21] that may alter their reactivity and chemoselectivity[14]. We evaluated the non-haem FePDP **4** catalyst (Fe(PDP)(SbF_6)$_2$), previously demonstrated to hydroxylate strong aliphatic C–H bonds[9,10], and its direct manganese analogue MnPDP **5** (Mn(PDP)(SbF_6)$_2$), each thought to proceed via metal(oxo) intermediates (Table 1, entries 7–8)[7,9–13]. Under

[1]Department of Chemistry, Roger Adams Laboratory, University of Illinois, Urbana, IL, USA. [2]Graduate School of Pharmaceutical Sciences, Kyoto University, Yoshida, Sakyo-ku, Kyoto, Japan. [3]Institute of Chemistry, University of Campinas, Campinas/SP, Brazil. *e-mail: mcwhite7@illinois.edu

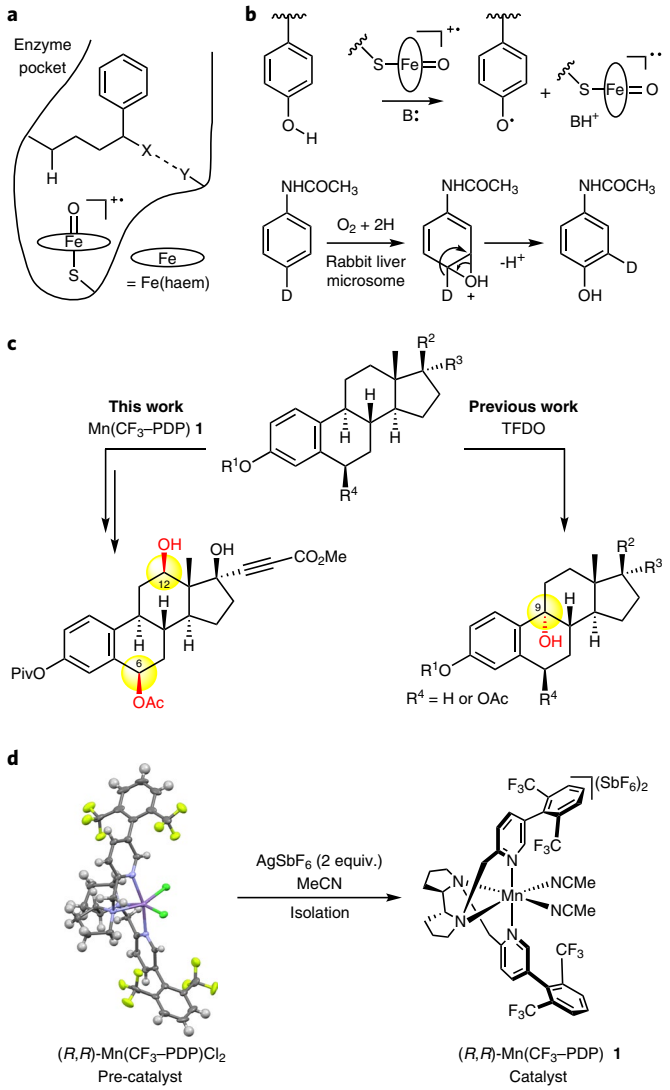

Fig. 1 | Enzymatic and small-molecule approaches for C–H oxidation. A chemoselective small-molecule catalyst capable of strong methylene C–H bond oxidations in the presence of the more oxidatively labile π-functionality of aromatic groups was previously unknown. **a**, Cytochrome P450 enzymes (CYPs) achieve such chemoselective oxidation of methylene C–H bonds by restricting the substrate's approach to the iron oxidant; however, these enzymes are challenging to use preparatively. **b**, The two major pathways of aromatic oxidation with the iron(oxo) oxidants generated in CYPs are electron transfer (top) or epoxidation followed by hydride shift (for example, the 'NIH shift', bottom). **c**, Small-molecule catalyst Mn(CF_3–PDP) **1** achieves chemoselective hydroxylation of strong methylene C–H bonds in the presence of aromatic functionalities. This reactivity is orthogonal to other oxidants that perform weaker bond oxidations (for example, benzylic C–H) in the presence of aromatic functionality, as demonstrated with an ethinylestradiol derivative (the site of oxidation is highlighted in yellow). **d**, The crystal structure of the Mn(CF_3–PDP)Cl_2 pre-catalyst shows the bulky ligand framework thought to be critical for the high chemoselectivity achieved with Mn(CF_3–PDP)$(CH_3CN)_2$·$(SbF_6)_2$ catalyst [Mn(CF_3–PDP)] **1.** CF_3-PDP, 1,1′-bis((5-(2,6-bis(trifluoromethyl)phenyl)pyridin-2-yl)methyl)-2,2′-bipyrrolidine.

Table 1 | Reaction development of Mn(CF_3–PDP) 1 catalysis

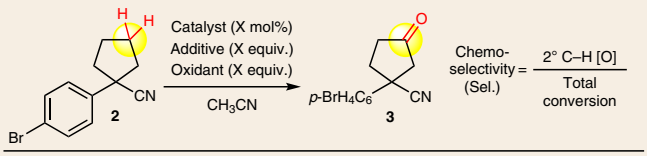

Entry	Catalyst	Additive	Oxidant	Temperature (°C)	Yield (%)	Sel. (%)
1	–	–	TFDO 3 equiv.	–20	Trace	ND
2	–	–	TFDO 3 (6) equiv.	0	Trace (11)	ND (18)
3	Ru(Me_3TACN) (2%)	–	CAN 2 x 3 equiv.	RT	Trace	ND
4	*cis*-Ru(dtbpy)$_2Cl_2$ (5%)	–	H_5IO_6 2 equiv.	RT	0	ND
5	Mn(OTf)$_2$, 0.1%; bipy, 1%	–	AcOOH 3 equiv.	RT	26	43
6	Mn(PDP)(OTf)$_2$ (0.1%)	CH_3COOH 14 equiv.	H_2O_2 2.5 equiv.	0	9	69
7	Fe(PDP) **4** (3×5%)	CH_3COOH 3×0.5 equiv.	H_2O_2 3×1.2 equiv.	RT[a]	1	2
8	Mn(PDP) **5** (3×5%)	CH_3COOH 3×0.5 equiv.	H_2O_2 3×1.2 equiv.	RT[a]	7	59
9	**5** (25%)	CH_3COOH 5 equiv.	H_2O_2 9 equiv.	RT[b]	36	71
10	Fe(CF_3-PDP) **6** (25%)	CH_3COOH 5 equiv.	H_2O_2 9 equiv.	RT[b]	24	27
11	Mn(CF_3-PDP) **1** (25%)	CH_3COOH 5 equiv.	H_2O_2 9 equiv.	RT[b]	21	95
12	**1** (25%)	$ClCH_2CO_2H$ 5 equiv.	H_2O_2 9 equiv.	RT[b]	73	90
13	**1** (25%)	Cl_2CHCO_2H 5 equiv.	H_2O_2 9 equiv.	RT[b]	66	77
14	**5** (25%)	$ClCH_2CO_2H$ 5 equiv.	H_2O_2 9 equiv.	RT[b]	32	65
15	**1** (10%)	$ClCH_2COOH$ 15 equiv.	H_2O_2 10 equiv.	0[c]	86	94
16	**5** (10%)	$ClCH_2COOH$ 15 equiv.	H_2O_2 10 equiv.	0[c]	38	85
17	**6** (10%)	$ClCH_2COOH$ 15 equiv.	H_2O_2 10 equiv.	0[c]	5	7
18	**1** (10%)	CH_3COOH 15 equiv.	H_2O_2 10 equiv.	0[c]	20	75

Isolated yields are an average of two (TFDO) or three (all catalytic reactions) runs. TFDO, methyl(trifluoromethyl)dioxirane; Me_3TACN, *N*,*N*′,*N*″-trimethyl-1,4,7-triazacyclononane; CAN, ceric ammonium nitrate; dtbpy, 4,4′-di-*tert*-butyl-2,2′-bipyridine; bipy, 2,2′-bipyridine; PDP, 1,1′-bis(pyridin-2-ylmethyl)-2,2′-bipyrrolidine; RT, room temperature. SbF_6-[hexafluoroantimony(v)] is used as counterion for catalyst **1**, **4**–**6**. [a]Iterative addition protocol; see ref. [9]. [b]Slow addition protocol; see ref. [28]. [c]Single catalyst addition (method A), standard procedure for Mn(CF_3–PDP) **1** used unless otherwise noted: substrate (0.3 mmol) with Mn(CF_3–PDP) **1** (0.03 mmol) and $ClCH_2CO_2H$ (4.5 mmol) dissolved in MeCN (0.6 ml) maintained at 0 °C, a solution of H_2O_2 (50% wt, 3.0 mmol) in MeCN (3.75 ml, 0.8 M) was added via syringe pump over 3 h.

analogous conditions, both catalysts proceeded with poor yields of the desired methylene oxidized products; however, in the case of the manganese catalyst, the chemoselectivity for the 2° oxidized product was significantly higher than that of its iron counterpart (entries 7–8). Although increased reactivity with similar chemoselectivity is observed by switching from the iterative addition protocol to the more forcing slow addition protocol, a preparatively useful yield could not be achieved (36% yield, entry 9).

We hypothesized that the restricted approach trajectory and enhanced electrophilicity provided to the metal(oxo) by appropriate ligand modifications could enhance chemoselectivity. A bulky, electrophilic metal(oxo) should prefer an electron-rich methylene C–H bond over a relatively electron-deficient and more sterically demanding π-system[15]. The sterically and electronically modified non-haem catalyst Fe(CF_3–PDP) **6** [Fe(CF_3–PDP)$(SbF_6)_2$] was reported to have preferential reactivity for methylene versus tertiary aliphatic C–H bonds[11]. We evaluated Fe(CF_3–PDP) **6** and its manganese analogue Mn(CF_3–PDP) **1** (Mn(CF_3–PDP)$(SbF_6)_2$) and found

that whereas both catalysts gave lower yields of **3** than Mn(PDP) **5** (entry 9), novel catalyst Mn(CF_3–PDP) **1** was unique in affording very high chemoselectivity (Table 1, entries 10–11). Site-selectivity trends analagous to those previously reported with Fe(CF_3–PDP) were observed[9–13], with Mn(CF_3–PDP) **1** favouring remote oxidation on the more sterically accessible methylene site (vide infra). Hyperconjugative activation by the alcohol of the methine C–H bond promotes subsequent oxidation to the ketone.

The electrophilicity of the presumed manganese oxo intermediate may also be tuned with the inclusion of acid additives, previously shown to modulate reactivity and selectivity with metal(oxo) species[22–25]. Acetic acid in non-haem iron-catalysed C–H oxidations enhances reactivity, probably by binding and delivery of a proton to the H_2O_2 at the metal centre to promote metal(oxo) carboxylate formation[9,23,26]. Carboxylic acid-containing substrates are able to direct C–H hydroxylations to electronically and sterically disfavoured sites, providing compelling evidence for carboxylate as an ancillary ligand to Fe(PDP) **4** during oxidation[24]. To probe this effect on the electronics of Mn(CF_3–PDP) **1**, we examined electron-deficient carboxylic acids in combination with **1**. We found that both chloro- and dichloroacetic acid significantly increased yields for methylene oxidation, but only chloroacetic acid maintained good chemoselectivities (Table 1, entries 12–13). Interestingly, chloroacetic acid did not show the same beneficial effect with the Mn(PDP) **5** catalyst for methylene oxidations (entry 14). Catalyst **1** loadings were decreased (25 mol% to 10 mol%) and the yield was enhanced by increasing the acid and H_2O_2 equivalents, decreasing the reaction temperature (room temperature → 0 °C) and modifying the addition protocol (entry 15, see Supplementary Table 1 for details). Under these optimized conditions, neither Mn(PDP) **5** nor Fe(CF_3–PDP) **6** showed significant improvements (entries 16–17), indicating that the catalyst is one critical component; however, switching back to acetic acid under these optimized conditions with **1** also led to significant diminishments in the yield and chemoselectivity for this oxidation (entry 18). Collectively, these results suggest a synergy between the acid additive and catalyst to furnish a remarkable amalgamation of reactivity and chemoselectivity.

Reaction scope. To assess the ability of aromatic groups to tolerate methylene oxidation reactions with **1**, we evaluated a cyclopentane substrate with electronically and sterically varied aromatic substituents (Table 2). A cyclopentane substrate with a phenyl substituent afforded poor yields of remote oxidation product **7** due to competitive aromatic oxidation. Consistent with the hypothesis that π-oxidation is more sterically demanding than C(sp^3)–H hydroxylation, introduction of an electron-rich but bulky *tert*-butyl (*t*-Bu) substituent blocks aromatic oxidation to afford desired methylene oxidation product **8** in 65% yield. Significantly, electron-rich and unsubstituted aromatic groups are also susceptible to CYP450 oxidations and this source of metabolic instability may account for the observation that approximately 50% of top leading drugs on the market are halogenated[4]. Mildly electron-withdrawing halogen-substituted aromatic groups are all well tolerated in this reaction: bromine ($\sigma_p = 0.23$), chlorine ($\sigma_p = 0.23$) and even fluorine ($\sigma_p = 0.06$) substituted substrates all afford synthetically useful yields of methylene oxidation products **3** (86%, Table 1, entry 15), **9** (81%, Table 2) and **10** (56%). It is worth noting that in gram-scale reactions, catalyst and acid loadings can be reduced to 5 mol% and 7.5 equiv., respectively, to afford products with comparable isolated yields and chemoselectivities (**9**, 72% yield, 84% chemoselectivity). The phthalimide group diminishes resonance donation of aniline, enabling effective remote methylene oxidation to furnish **11** in 63% yield. Compounds with *meta*-ester ($\sigma_m = 0.23$) and 3,5-difluoro substituents are oxidized with Mn(CF_3–PDP) **1** to give **12** (73%) and **13** (66%) in useful yields. When evaluating aromatic substrates with stronger electron-withdrawing substituents such as *para*-esters and nitriles, somewhat tolerated with Fe(CF_3–PDP) **6**, we see that **1** affords higher yields of methylene oxidized products **14** and **15** with excellent chemoselectivity. Underscoring the unprecedented level of chemoselectivity with the new Mn(CF_3–PDP) **1**, direct comparisons made with Fe(CF_3–PDP) **6** under previously reported optimal conditions (Table 1, entry 10) show that **1** gives significant improvements in yields and selectivities relative to **6** (11% yield for **12** and **13**, 28% for **14**, 55% for **15**). Substrates with trifluoromethoxy and difluoromethoxy aromatic groups, increasingly found in pharmaceuticals[2], afford remote methylene oxidation in 77% (**16**) and 55% (**17**) yields, respectively. Cyclopentanes with a nitrophthalimide masked primary amine as well as isobenzofuranone and oxindole cores, seen in fluorescein and sunitinib, afforded remote methylene oxidation products **18**, **19** and **20** in good yields and chemoselectivities. Spirocycle substrates are not uniquely effective; methylene oxidations of analogous aromatic compounds containing remotely appended cyclopentane rings and linear aliphatic chains afford products in good yields (64% for **21**, 61% for **22**, 82% for **23**; vide infra). Following site-selectivity rules established with analogous non-haem iron catalysts[9–13], oxidation by **1** of a 3-butyl 3-acetoxy oxindole substrate gave only one observed methylene oxidized product at the most sterically accessible and electron-rich δ site remote from the tertiary acetoxyl moiety (**22**). When the alkyl chain was extended by one carbon in an *N*-pentyl benzenesulfonamide substrate, a 3:1 δ:γ mixture of oxidized products (**23**) was observed, still favouring the most remote δ site.

Small-ring carbocycles are increasingly being utilized in pharmaceutical compounds to address the physicochemical and pharmacological challenges in classic sp^2-hybridized planar structures[27]. Cyclohexyl rings are oxidized in good yields, but with poor site-selectivities (Table 2, **24**, 1:1 γ:δ ratio) due to competing electronic effects favouring the remote δ site and stereoelectronic effects (that is, relief of ring strain) favouring the γ site[9–13]. Despite their prevalence in natural products and pharmaceutical molecules, cyclobutanes are rarely demonstrated in intermolecular C–H oxidations due to the partial sp^2-hybridized character of the C–H bonds. Under Mn(CF_3–PDP) **1** catalysis, remote cyclobutyl groups are effectively oxidized in preparative yields with excellent site-selectivity (**25**). The chemoselectivity and high yield of remote oxidation are maintained in reactions with a series of biaryl bioactive molecule derivatives, further highlighting the generality of this method. A cyclobutyl analogue of the pesticide proclonol is oxidized on the cyclobutyl ring in good yield and site-selectivity (**26**, 52% yield, 4:1 δ:γ). A derivative of clorindione, a vitamin K antagonist, is oxidized with **1** to afford 60% isolated yield of ketone product **27**. A derivative of non-steroidal anti-inflammatory drug ketoprofen affords remote ketone products **28** in 52% yield and 9:1 site-selectivity.

The site-selectivity of Mn(CF_3–PDP) **1** catalysis, analogous to that reported for Fe(PDP) and Fe(CF_3–PDP) catalysis, is not solely dependent on the BDEs of the C–H bond: in the **1**-catalysed oxidation of dichlorobenzylketone derivative, C–H oxidation of the remote methylene sites on the cyclopentyl ring are preferred over oxidation of weaker benzylic and tertiary sites that are electronically deactivated by the proximal carbonyl (Table 2, **29**). Highlighting the orthogonality of Mn(CF_3–PDP) **1** catalysis to alternative methods, **1** preferentially oxidizes at the less electron-rich but more sterically accessible methylene sites to afford **30** and **31**, whereas electrochemical radical methods[18] and TFDO[17] both afford the tertiary alcohol as the exclusive or major product. Cyclopropanes effectively activate α-methylene sites towards oxidation with **1** to afford a 54% combined yield of ketone and alcohol products **32** with no detectable ring-opened products. In contrast, other Mn catalysts, including Mn(PDP)$(OTf)_2$ (ref. [8]) are reported to give no product or trace yields.

Medicinally interesting compounds often contain aromatic rings with varied electronic and steric properties (Table 2). Whereas the

Table 2 | Substrate scope of Mn(CF$_3$-PDP) 1 catalysed chemoselective C–H hydroxylation

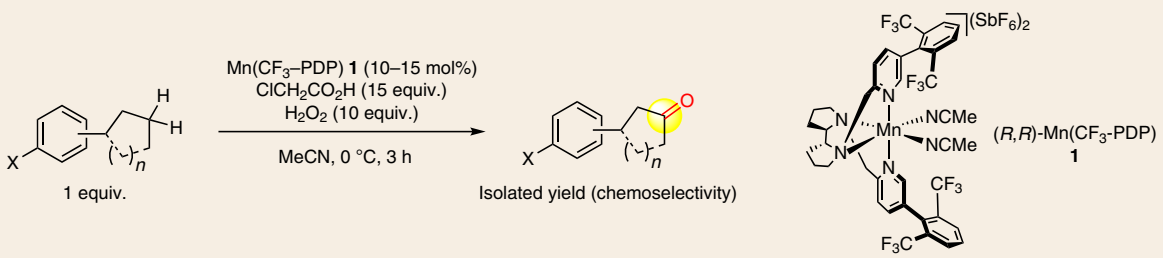

Aromatic substrates

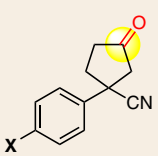

X = H **7**, 10% (12%)
t-Bu **8**, 65% (73%)
Cl **9**, 81% (89%)
Gram scale 72% (84%)
(5 mol% **1**)
F **10**, 56%[a] (63%)
NPhth **11**, 63% (78%)

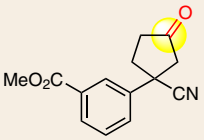

12, 73% (87%)
Cat. **6**[b]: 11% (11%)

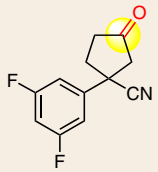

13, 66% (82%)
Cat. **6**[b]: 11% (18%)

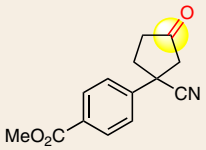

14, 84% (95%)
Cat. **6**[b]: 28% (30%)

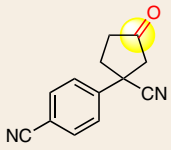

15, 72% (90%)
Cat. **6**[b]: 55% (60%)

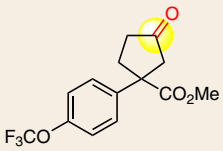

16, 77%[a] (77%)

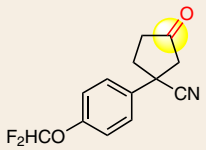

17, 55%[a] (55%)

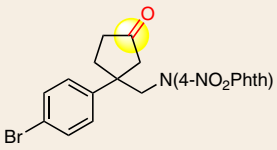

18, 60% (67%)

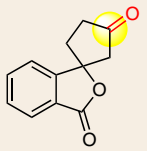

19, 62% (69%)

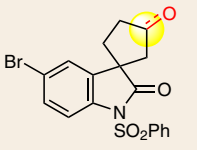

20, 52%[c] (66%) 2:1 K:A

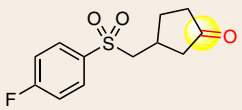

21, 64% (64%)

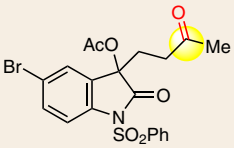

22, 61%[a] (72%)

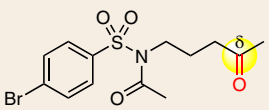

23, 82% (91%) 3:1 δ:γ

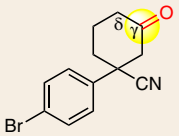

24, 64% (78%) 1:1 γ:δ[d]

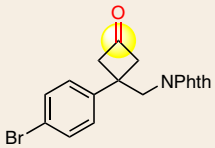

25, 57%[a] (69%)

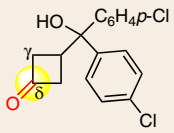

26, 52% (52%) 4:1 δ:γ[d]

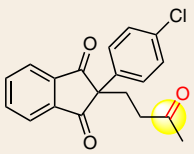

27, 60% (70%)

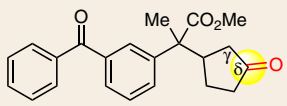

28, 52% (52%) 9:1 δ:γ

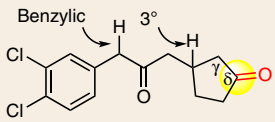

29, 53% (53%) 3:1 δ:γ

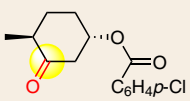

30, 58% 1.2:1 2°:3°
Electrochemical: 56% 3°, 1:1 d.r.

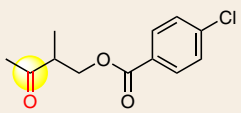

31, 58% 2:1 2°:3°
TFDO: 66% 1:2 2°:3°

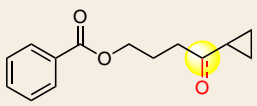

32, 54%[e] 4.5:1 K:A
Mn(PDP)(OTf)$_2$: 0%; **Mn(OTf)$_2$/bipy**:17%

Aromatic substrates with multiple substitutions of varied electronic and steric properties

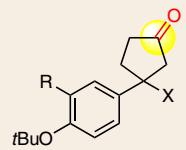

R = H **X** = CN **33**, 0% (0%)
Cl CO_2Me **34**, 73% (73%)

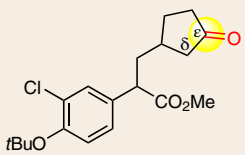

35, 54% (60%) 3.5:1 ε:δ

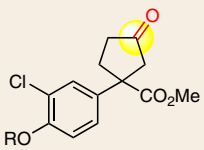

R = CH_3 **36**, 35% (42%)
CD_3 **37**, 41% (46%)

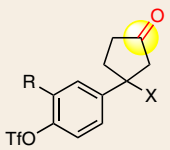

R = OMe **X** = CO_2Me **38**, 52% (57%)
CH_3 CN **39**, 59% (75%)

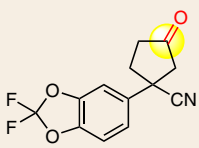

40, 55% (76%)

Method A is used unless otherwise noted. Isolated yields are the average of two to three runs. Site of oxidation is highlighted in yellow. Chemoselectivity (2° C–H [O]/total conversion) is given in parentheses. NPhth, phthalimide; N(4-NO_2Phth), 4-nitrophthalimide. [a]Iterative catalyst addition protocol (method B): a total of 15 mol% Mn(CF$_3$-PDP) **1** was added in three portions (5 mol%, three times). See Methods for more details. [b]25 mol% Fe(CF$_3$-PDP) **6**, slow addition protocol (ref. [25]). [c]Starting material recycled once. Ketone to alcohol ratio reported as K:A. [d]Ratios are statistically corrected. [e]7% chloroacetic ester, 8% recovered starting material also observed.

tert-butoxybenzene moiety in the precursor of **33** is oxidized, addition of a bulky, electron-withdrawing chlorine substituent to the aromatic group affords methylene oxidized product **34** in 73% yield. A compound of alternative topology with the same aromatic substitution is also oxidized in preparative yields to afford **35** in 54% yield, albeit in diminished site-selectivity (3.5:1 ε:δ). Replacing O*t*-Bu

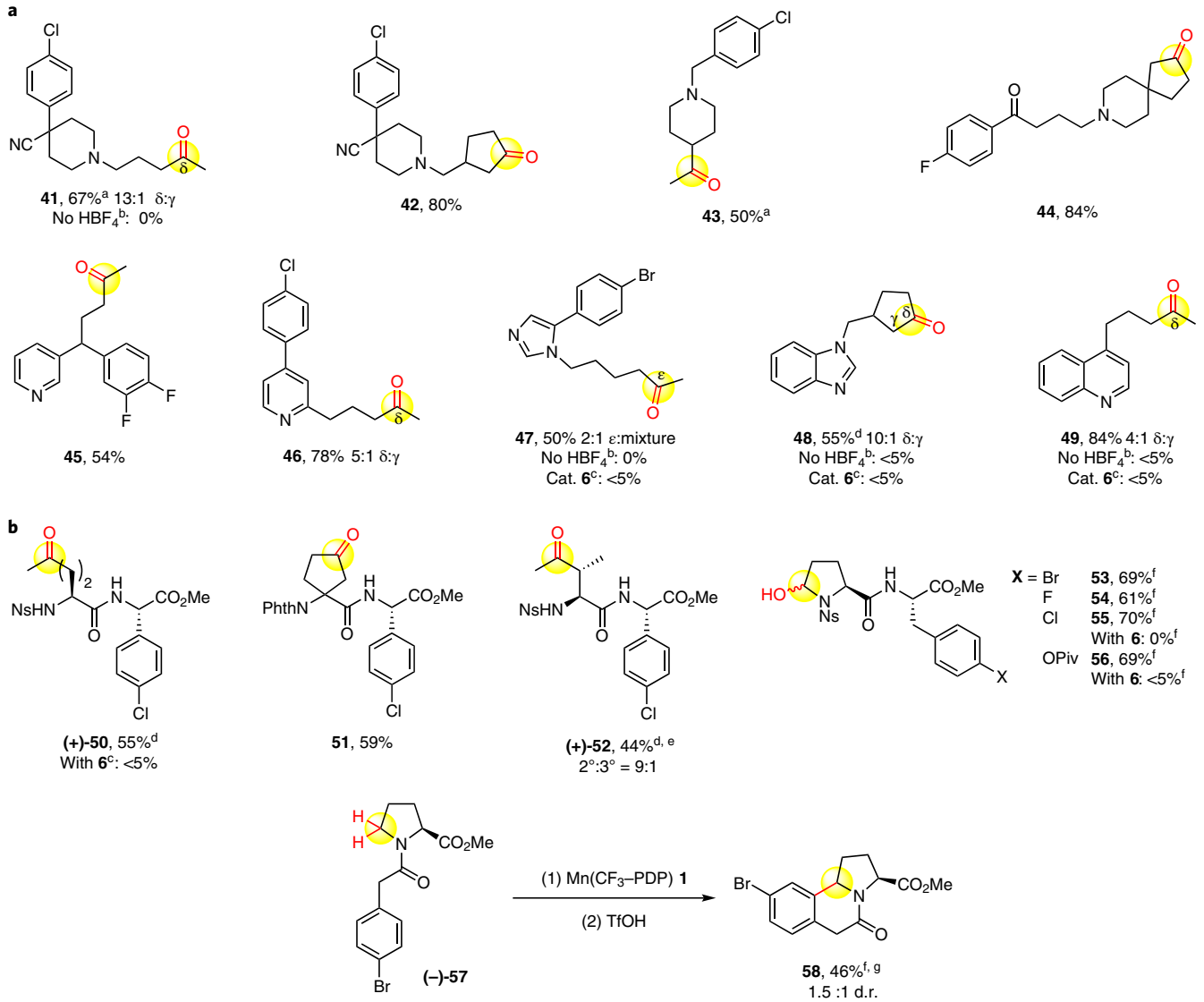

Fig. 2 | Chemoselective methylene C–H oxidation. a, Mn(CF_3–PDP) **1** catalysed remote 2° C–H oxidation in the presence of aromatic functionality with basic nitrogen-containing heterocycles or heteroaromatics. Unless otherwise noted, basic nitrogen was HBF_4·OEt_2 protected as described in ref. [28] followed by slow catalyst addition protocol (Method C) at −36 °C where both H_2O_2 (10 equiv.) and Mn(CF_3–PDP) **1** (10 mol%) were simultaneously added over 3 h. See Methods for more details. **b**, Mn(CF_3–PDP) **1** oxidation of peptides containing amino acids with mildly deactivated aromatic groups. This enables intramolecular functionalizations with arene π-nucleophiles to furnish medicinally relevant tricyclic cores. HBF_4·OEt_2 complexation was not used on peptide substrates. Isolated yields are the average of two to three runs. Site of oxidation is highlighted in yellow. Ns; 4-nitrophenylsulfonyl. [a]Method C used at 0 °C. [b]Without HBF_4 complexation with **1** under the same conditions used with complexation (Method B or C). [c]25 mol% Fe(CF_3–PDP) **6**, slow addition protocol[28]. [d]Method B used. [e]Starting material recycled once. [f]Method A used with AcOH (15 equiv.) and H_2O_2 (5.0 or 7.5 equiv.) at −36 °C. [g]Crude hemiaminal, TfOH (2.0 equiv.), 90 °C, 2 h.

with OMe in the substrate followed by oxidation with **1** provides product **36** in diminished yield and selectivity. Consistent with the lability of the ethereal site, oxidation by **1** of an analogous deuterated anisole compound affords **37** with a slightly higher yield and chemoselectivity. As the aromatic ring is made more electron-deficient, ethereal and benzylic C–H bonds are shielded from oxidation with **1**: in triflate protected phenol substrates with methyl and methoxyl substituents, higher yields and selectivities are obtained for methylene oxidized products **38** and **39**, respectively. In a difluorobenzodioxole substrate where the ethereal C–H bonds are replaced with fluorine and the π-donation of the oxygen into the aromatic ring is attenuated, remote oxidized product **40** is furnished in preparative yields.

A cursory glance at pharmaceutical molecules reveals that the combination of halogenated aromatics and nitrogen heterocycles (for example, piperidines, pyridines and imidazoles) is ubiquitous in their structures[1,2]. We explored Mn(CF_3–PDP) **1** catalysis with the known HBF_4 protection strategy for enabling remote methylene C–H oxidations in the presence of basic nitrogen heterocycles that additionally contain aromatic moieties (Fig. 2a)[28]. 4-Arylpiperidines and benzyl-derived piperidines, prevalent motifs in opioid analgesics and cognition enhancing drugs (for example, ketobemidone and donepezil), were tolerated and afforded remote methylene oxidized products in good yields (**41**–**43**). In the absence of HBF_4, no desired remote oxidation was observed, indicating the chloroacetic acid alone is not effective in protecting the basic amine func-

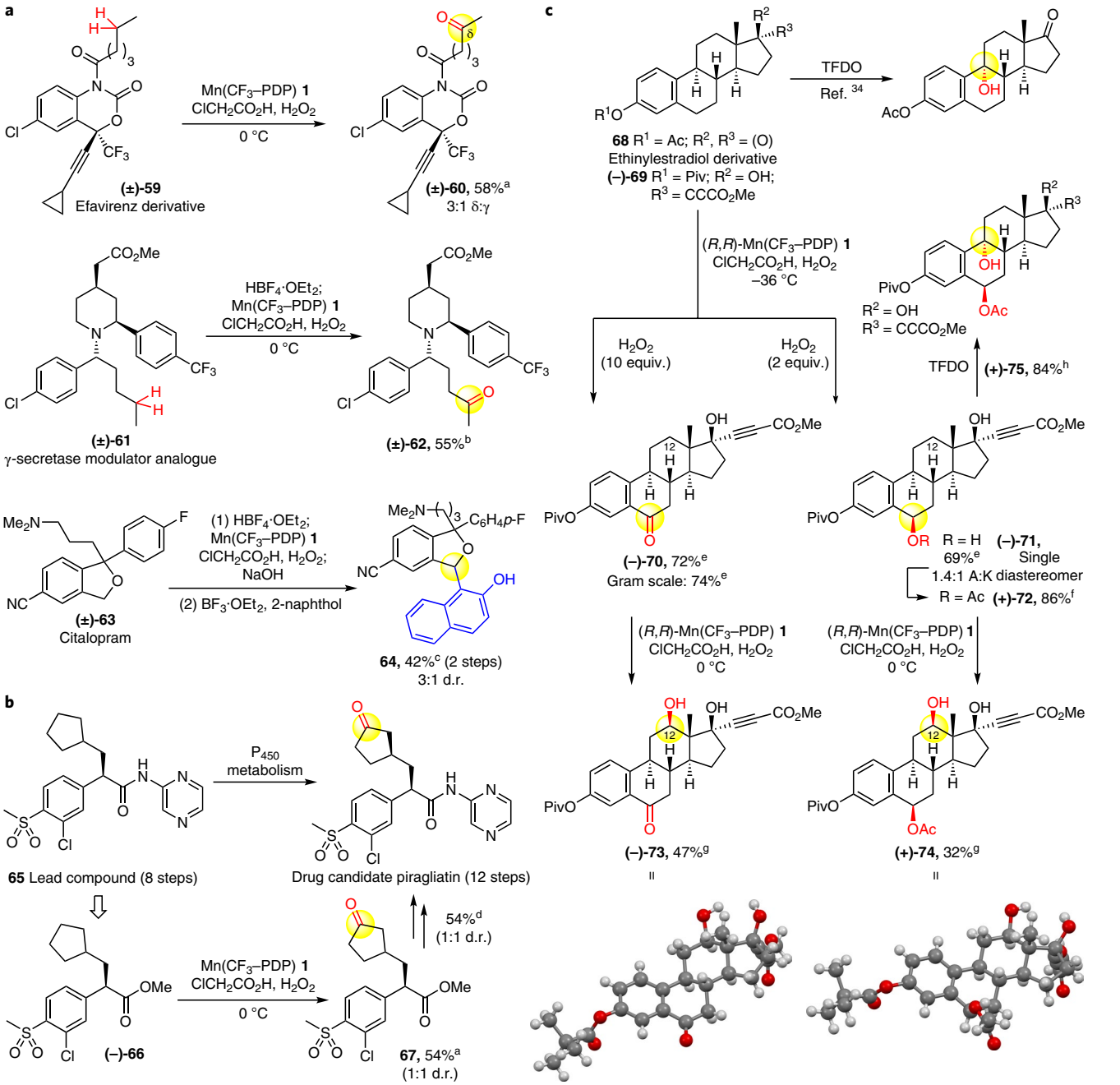

Fig. 3 | Late-stage methylene hydroxylation of synthetic and natural product, aromatic drugs derivatives. a, Derivatives of the HIV-1 drug efavirenz and a γ-secretase modulator analogue that house oxidatively sensitive π-functionality, such as aryl halides, acetylenes, piperidine and tertiary amines are oxidized with Mn(CF_3–PDP) **1** at remote methylene sites in preparative yields. Antidepressant citalopram is oxidized to a hemiacetal and arylated with an arene π-nucleophile via an intermediate oxocarbenium. **b**, Drug candidate piragliatin, identified as a metabolite of drug lead **65**, required de novo synthesis to furnish quantities for further evaluation. Mn(CF_3–PDP) **1** catalysis enables an advanced lead intermediate to be rapidly transformed to piragliatin. **c**, Sequential Mn (CF_3–PDP) **1** catalysed 2° benzylic/2° aliphatic C–H oxidation of an ethinylestradiol derivative. 2° benzylic oxidation can be tuned with oxidant to give ketone **70** or diastereomerically pure alcohol **71**, which undergo further diastereoselective C12 β methylene hydroxylation to alcohols **73** and **74** (crystal structures confirm the 12β configuration). In contrast, TFDO furnishes oxidation at the doubly activated 3° benzylic site. All reactions run with limiting substrate and isolated yields reported as an average (two to three reactions, using **1**). See Supplementary Sections VIII and IX for more details. Ac, acetyl; Piv, pivaloyl. [a]Method A used at 0 °C. [b]HBF_4·OEt_2 protected ref. [28], followed by method C at 0 °C. [c]Method A using 2 equiv. H_2O_2; arylation protocol, ref. [29]. [d]LiOH·H_2O (5 equiv.); oxalyl chloride (1.1 equiv.); 2-aminopyrazine (2.2 equiv.), pyridine (2.2 equiv.). [e]Method A with modifications: **1** (5 mol%; 2 mol% for gram scale), $ClCH_2CO_2H$ (7.5 equiv.), H_2O_2 (10 equiv. for **70** or 2 equiv. for **71**), 4:1 MeCN:CH_2Cl_2 at −36 °C. [f]Ac_2O (2.4 equiv.), NEt_3 (2.4 equiv.), CH_2Cl_2, 86%. [g]Method A with 4:1 MeCN:CH_2Cl_2 at 0 °C. [h]TFDO: **72** (0.05 mmol) in CH_2Cl_2 (0.5 ml) at −20 °C. TFDO (0.4 M solution, 0.25 ml, 2 equiv.) added at −20 °C and stirred for 40 min in dark.

tionality. An analogue of haloperidol bearing 4-fluorophenyl butyl ketone and piperidine pharmacophores undergoes remote oxidation with **1** in 84% isolated yield to afford **44**. An aliphatic motif with a 1,1-disubstituted pyridine-aryl pharmacophore is effectively oxidized to afford ketone product **45** in 54% yield. Mn(CF_3–PDP) **1** oxidation of a chloro-phenylpyridine substrate shows excellent

yields (**46**, 78%) and good site-selectivity (5:1 δ:γ). Additionally, imidazole, benzimidazole and quinoline derivatives are successfully oxidized to afford remote ketone in 50% (**47**), 55% (**48**) and 84% (**49**) yields, respectively. Significantly, without the combination of HBF_4 protection and Mn(CF_3–PDP) **1** catalysis, no significant remote oxidized products were observed: **1** affords enhanced heterocycle tolerance relative to iron catalyst **6**, but the protonation strategy is still necessary in oxidations with **1** for less basic heterocycles to access **47**, **48** and **49**.

Previous reports demonstrated an impressive ability of iron catalysts to afford remote aliphatic C–H hydroxylations on peptides[29]. However, the aromatic side chains present were restricted to strongly electron-withdrawing triflate ($\sigma = 0.53$) protected tyrosine. Using Mn(CF_3–PDP) **1** catalysis, dipeptide-containing chlorophenylglycin residues can be oxidized at aliphatic norleucine and cyclopentyl residues to afford a single oxidation product in 55% (**50**) and 59% (**51**) yields, respectively (Fig. 2b). An isoleucine residue is selectively oxidized at the more sterically accessible methylene site to furnish **52** with 9:1 secondary:tertiary ratio. Mn(CF_3–PDP) **1** selectively installs the diversifiable C5-hydroxyl group onto proline in dipeptide settings containing halogenated phenylalanine and now readily removable pivalate-protected tyrosine amino acid residues in good yields (**53**–**56**). Arene π-nucleophiles can now be linked directly to an amide nitrogen (**57**) before C–H hydroxylation to enable *N*-acyl iminium intramolecular cyclization to furnish tricyclic isoquinolone derivative **58**. Importantly, in all cases examined Fe(CF_3–PDP) **6** oxidations run under their reported optimal conditions do not tolerate these aromatic functionalities and afford only trace remote oxidized products (for example, **50**, **55** and **56**).

Late-stage oxidation of pharmaceuticals. The unprecedented chemoselectivity and reactivity of Mn(CF_3–PDP) **1** for remote methylene oxidations in the presence of pharmaceutically relevant aromatics and heteroaromatic moieties provides an opportunity to effect late-stage diversification of drug leads (Fig. 3a). The atomistic change of C–H to C–O is a validated way to impact physiological responses of small molecules due to altered interactions with proteins and/or changes to physical properties. Evaluation of the hexanoyl derivative **59** of efavirenz, a WHO essential medicine for HIV-1, demonstrates that the singular chemoselectivity of **1**-catalysed aliphatic C–H oxidation persists in the presence of the π-system of an aromatic and an alkyne moiety to furnish **60** in 58% yield with no observed products from oxidation of the aromatic or alkyne functionality. Compound **61**, a γ-secretase modulator analogue[30], was effectively oxidized by the **1**/HBF_4 strategy to give remote ketone product **62** in 55% yield. The activated tertiary benzylic sites, generally susceptible to TFDO and radical-mediated C–H abstraction, did not undergo oxidation or epimerization with **1**. Antidepressant citalopram **63**, housing two aromatic rings and a tertiary amine, underwent selective C–H hydroxylation alpha to the ethereal oxygen. Treatment of the hemiacetal with $BF_3{\cdot}Et_2O$ furnished a reactive oxocarbenium ion intermediate that underwent diastereoselective nucleophilic attack by an electron-rich arene to furnish the 2-naphthol adduct **64** in 42% overall yield (two steps, 3:1 d.r.). Significantly, generation of hemiacetals has not been described under iron catalysis, probably because the highly reactive hemiacetal rapidly undergoes further oxidation to a carbonyl.

Oxidative metabolism of pharmaceuticals via CYP450 enzyme-mediated C–H hydroxylation is a major pathway for drug clearance in vivo, and their identification is crucial for evaluation of their safety and effectiveness[31]. Piragliatin, a drug candidate advanced in the clinic for type 2 diabetes, was discovered via in vivo metabolite studies (MetID) of lead compound **65** (Fig. 3b)[32]. Because MetID studies only generate analytical amounts of the metabolite, piragliatin and its diastereomer, as well as several other potential cyclopentyl ring metabolites, were produced in quantities needed for identification and in vivo safety and efficacy profiling via independent total syntheses that each proceeded with higher step counts than that of the lead **65** (eight steps). Advanced synthetic intermediate **66**, whose acid was used in the synthesis of **65**, can be intercepted and directly oxidized with **1** to afford the C3 ketone **67** (1:1 d.r.) in 54% yield. Hydrolysis of methyl ester followed by amide coupling with 2-aminopyrazine rapidly affords piragliatin and its diastereomer (54% yield, 1:1 d.r.)[32]. Mn(CF_3–PDP) **1** catalysis may provide a powerful means for rapidly accessing aliphatic metabolites of aromatic drugs in preparative quantities.

Sequential C–H oxidation of complex natural products. Natural products (for example, polyketides, steroids and flavonoids) containing aromatic moieties showcase a wide range of biological activities and serve as impacting starting points for generating new pharmaceuticals[3,33]. Chemical modifications to these complex structures are generally limited to manipulations of native functionality. We envisioned that Mn(CF_3–PDP) **1** might be used on medicinally important aromatic steroids such as oestrogen supplement ethinylestradiol, containing a sensitive aromatic ring and an alkyne, to enable the rapid, sequential build-up of remote hydroxylation on a steroid core (Fig. 3c). In contrast to TFDO, which hydroxylates the doubly activated tertiary benzylic site on oestrone derivatives (for example, **68**)[34], performing oxidation with **1** on ethinylestradiol derivative **69** effectively oxidizes the sterically more accessible secondary benzylic C–H site in high yields. The oxidation state of the newly formed C–O bond is controlled by the amount of hydrogen peroxide oxidant: 10 equiv. affords benzylic ketone product **70** (72% yield; gram-scale synthesis with 2% of **1**, 74% yield), whereas 2 equiv. affords a mixture of ketone **70** and alcohol **71**, formed as a single diastereomer. Further hydroxylation at the non-activated methylene C12 position can be effected with **1** to afford diastereomerically pure alcohol products: oxidation of ketone **70** and the protected benzylic alcohol **72** afford single diastereomers of C12 β-alcohol in 47% yield of **73** and 32% yield of **74**. The observed diastereoselectivity and absence of over-oxidized C12 ketone products is probably due to the inability of bulky catalyst **1** to access the sterically hindered C12 hydrogen. In sharp contrast, TFDO oxidation of **72** led to hydroxylation at the tertiary benzylic site to afford **75** in 84% yield. The ability to access hydroxylation of methylene sites on steroids has been primarily limited to enzymes and engineered directing group approaches[35,36]. Despite the fact that C12 hydroxylation occurs in numerous classes of natural steroids (for example, polyoxypregnanes, digoxigenin and cholic acid), it is significant to note that the only non-directed C–H hydroxylations at this methylene position, and others, have been effected with (PDP)-inspired small molecule catalysts[28,37,38].

Conclusion

Recognition of the benefits of moving away from flat architectures in drug design is stimulating the incorporation of more C(sp^3)–H bonds into aromatic medicinal compounds. The development of the chemoselective and reactive Mn(CF_3–PDP) **1** catalyst system described herein enables the strategic advantages of late-stage aliphatic C–H oxidation to be leveraged in these settings. Following the same predictable selectivity rules first established with Fe(PDP) and Fe(CF_3–PDP) catalysts, the Mn(CF_3–PDP) **1** catalyst system site-selectively oxidizes methylene sites distinguished by subtle differences in electronic, steric and stereoelectronic environments in a range of carbocyclic and linear alkane structures. In sharp contrast to all previous small-molecule C–H oxidation systems, Mn(CF_3–PDP) **1** affords preparative methylene oxidations in medicinally relevant aromatic compounds substituted with halogen, oxygen, nitrogen, heterocyclic and biaryl moieties. We anticipate that this discovery will benefit future catalyst design in developing chemoselective and reactive aliphatic C–H oxidation catalysts. Additionally,

small-molecule therapeutics will be empowered with **1** to rapidly diversify aromatic drugs and natural products and quickly identify their metabolites. Future studies will probe the mechanism that biases the relatively simple Mn(CF_3–PDP) **1** catalyst system towards methylene C–H oxidation and impedes non-productive aromatic oxidation.

Methods

Method A: single catalyst addition protocol. A 40 ml vial was charged with substrate (0.3 mmol, 1.0 equiv.), Mn(CF_3–PDP) **1** (0.03 mmol, 10 mol%), $ClCH_2CO_2H$ (425 mg, 4.5 mmol, 15.0 equiv.) and a stir bar. Acetonitrile (MeCN, 0.6 ml, 0.50 M) was added along the wall to ensure all compounds were washed beneath the solvent level and the vial was sealed with a screw cap fitted with a polytetrafluoroethylene (PTFE)/silicone septum. The vial was cooled to 0 °C with an ice/water bath. A separate solution of H_2O_2 ((204 mg, 3.0 mmol, 10.0 equiv.), 50% (wt) in H_2O, purchased from Sigma-Aldrich) in MeCN (3.75 ml) was loaded into a 10 ml syringe fitted with a 25 G needle and added dropwise to the stirring reaction over 3 h via a syringe pump (1.25 ml h^{-1} addition rate) while maintaining the reaction vial at 0 °C. On completion, the reaction mixture was concentrated to a minimum amount of solvent. The residue was dissolved in ~20 ml dichloromethane (DCM) and washed with 9 ml sat. $NaHCO_3$ solution (caution: CO_2 released) to remove $ClCH_2CO_2H$. The aqueous layer was extracted with ~15 ml DCM twice and the combined organic layer was dried with Na_2SO_4. The filtrate was concentrated and purified by flash chromatography on silica gel.

Method B: iterative catalyst addition protocol. A 40 ml vial was charged with substrate (0.3 mmol, 1.0 equiv.), Mn(CF_3–PDP) **1** (0.015 mmol, 5 mol%), $ClCH_2CO_2H$ (425 mg, 4.5 mmol, 15.0 equiv.) and a stir bar. MeCN (0.6 ml, 0.50 M) was added along the wall to ensure all compounds were washed beneath the solvent level and the vial was sealed with a screw cap fitted with a PTFE/silicone septum. The vial was cooled to −36 °C with a 1,2-dichloroethane/dry ice bath or to 0 °C with an ice/water bath. A separate solution of H_2O_2 (204 mg, 3.0 mmol, 10.0 equiv.; 50% (wt) in H_2O, purchased from Sigma-Aldrich) in MeCN (3.75 ml) was loaded into a 10 ml syringe fitted with a 25 G needle and added dropwise to the stirring reaction over 3 h via a syringe pump (1.25 ml h^{-1} addition rate) while maintained at the initial temperature set for the reaction (−36 °C or 0 °C). The initial time was recorded as the time the first drop of H_2O_2 solution was added into the reaction. One hour after the initial time, another batch of catalyst (0.015 mmol, 5 mol%) was dissolved with 0.1 ml MeCN in a 0.5-dram vial and added dropwise into the reaction via syringe followed directly by another 0.1 ml MeCN (used to rinse the vial). The addition of 5 mol% catalyst was repeated 2 h after the initial time using the same procedure. A total of 15 mol% of catalyst was used in this protocol. On completion, the reaction was worked up and purified as described in method A.

Method C: slow catalyst addition protocol. A 40 ml vial was charged with substrate (0.3 mmol, 1.0 equiv.), $ClCH_2CO_2H$ (425 mg, 4.5 mmol, 15.0 equiv.) and a stir bar. MeCN (0.6 ml, 0.50 M) was added along the wall to ensure all compounds were washed beneath the solvent level and the vial was sealed with a screw cap fitted with a PTFE/silicone septum. The vial was cooled to −36 °C with a 1,2-dichloroethane/dry ice bath or to 0 °C with an ice/water bath. A 1.0 ml syringe was filled with a solution of Mn(CF_3–PDP) **1** (0.03 mmol, 10 mol%) in MeCN (0.375 ml, 0.083 M). A few drops of this solution were added to the reaction. A 10 ml syringe was filled with a solution of H_2O_2 (204 mg, 3.0 mmol, 10.0 equiv.; 50% wt in H_2O, purchased from Sigma-Aldrich) in MeCN (3.75 ml, 0.8 M). Both syringes were fitted with 25 G needles and loaded onto a syringe pump, providing a slow simultaneous addition of catalyst and oxidant solutions over 3 h while maintaining the initial temperature set for the reaction (−36 °C or 0 °C) (1.25 ml h^{-1} addition rate for the H_2O_2 syringe; 0.125 ml h^{-1} for the catalyst syringe). On completion, the reaction was worked up and purified as described in method A.

Synthetic procedures for Mn(CF_3–PDP) **1** and for all substrates in the manuscript are provided in Supplementary Sections II–IX.

Data availability

Crystallographic data for the structures reported in this Article have been deposited at the Cambridge Crystallographic Data Centre (CCDC) under deposition nos. CCDC 1869257 for (*S*,*S*)-**5**, CCDC 1869258 for **73**, CCDC 1869259 for **74** and CCDC 1869260 for (*R*,*R*)-**S2**. Copies of the data can be obtained free of charge from www.ccdc.cam.ac.uk/structures/. All other data supporting the findings of this study are available within the Article and its Supplementary Information, or from the corresponding author upon reasonable request.

Received: 25 August 2018; Accepted: 18 October 2018;
Published online: 17 December 2018

References

1. Blakemore, D. C. et al. Organic synthesis provides opportunities to transform drug discovery. *Nat. Chem.* **10**, 383–394 (2018).
2. Cernak, T., Dykstra, K. D., Tyagarajan, S., Vachal, P. & Krska, S. W. The medicinal chemist's toolbox for late stage functionalization of drug-like molecules. *Chem. Soc. Rev.* **45**, 546–576 (2016).
3. McMurray, L., O'Hara, F. & Gaunt, M. J. Recent developments in natural product synthesis using metal-catalysed C–H bond functionalisation. *Chem. Soc. Rev.* **40**, 1885–1898 (2011).
4. Ford, M. C. & Ho, P. S. Computational tools to model halogen bonds in medicinal chemistry. *J. Med. Chem.* **59**, 1655–1670 (2016).
5. Ortiz de Montellano, P. R. (ed.) *Cytochrome P450: Structure, Mechanism, and Biochemistry* (Springer, Berlin, 2015).
6. Mack, J. B. C., Gipson, J. D., Du Bois, J. & Sigman, M. S. Ruthenium-catalyzed C–H hydroxylation in aqueous acid enables selective functionalization of amine derivatives. *J. Am. Chem. Soc.* **139**, 9503–9506 (2017).
7. Ottenbacher, R. V., Samsonenko, D. G., Talsi, E. P. & Bryliakov, K. P. Highly efficient, regioselective, and stereospecific oxidation of aliphatic C–H groups with H_2O_2, catalyzed by aminopyridine manganese complexes. *Org. Lett.* **14**, 4310–4313 (2012).
8. Adams, A. M., Du Bois, J. & Malik, H. A. Comparative study of the limitations and challenges in atom-transfer C–H oxidations. *Org. Lett.* **17**, 6066–6069 (2015).
9. Chen, M. S. & White, M. C. A predictably selective aliphatic C–H oxidation reaction for complex molecule synthesis. *Science* **318**, 783–787 (2007).
10. Chen, M. S. & White, M. C. Combined effects on selectivity in Fe-catalyzed methylene oxidation. *Science* **327**, 566–571 (2010).
11. Gormisky, P. E. & White, M. C. Catalyst-controlled aliphatic C–H oxidations with a predictive model for site-selectivity. *J. Am. Chem. Soc.* **135**, 14052–14055 (2013).
12. White, M. C. Adding aliphatic C–H bond oxidations to synthesis. *Science* **335**, 807–809 (2012).
13. White, M. C. & Zhao, J. Aliphatic C–H oxidations for late-stage functionalization. *J. Am. Chem. Soc.* **140**, 13988–14009 (2018).
14. Paradine, S. M. et al. A manganese catalyst for highly reactive yet chemoselective intramolecular C(sp^3) –H amination. *Nat. Chem.* **7**, 987–994 (2015).
15. Padwa, A. et al. Ligand effects on dirhodium(II) carbene reactivities. Highly effective switching between competitive carbenoid transformations. *J. Am. Chem. Soc.* **115**, 8669–8680 (1993).
16. Quinn, R. K. et al. Site-selective aliphatic C–H chlorination using *N*-chloroamides enables a synthesis of chlorolissoclimide. *J. Am. Chem. Soc.* **138**, 696–702 (2016).
17. Asensio, G., Castellano, G., Mello, R. & González Núñez, M. E. Oxyfunctionalization of aliphatic esters by methyl(trifluoromethyl)dioxirane. *J. Org. Chem.* **61**, 5564–5566 (1996).
18. Kawamata, Y. et al. Scalable, electrochemical oxidation of unactivated C–H bonds. *J. Am. Chem. Soc.* **139**, 7448–7451 (2017).
19. Yosca, T. H. et al. Iron(IV)hydroxide pK_a and the role of thiolate ligation in C–H bond activation by cytochrome P450. *Science* **342**, 825–829 (2013).
20. Guroff, G. et al. Hydroxylation-induced migration. The NIH shift: recent experiments reveal an unexpected and general result of enzymatic hydroxylation of aromatic compounds. *Science* **157**, 1524–1530 (1967).
21. Jeon, S. & Bruice, T. C. Redox chemistry of water-soluble iron, manganese, and chromium metalloporphyrins and acid–base behavior of their lyate axial ligands in aqueous solution: influence of electronic effects. *Inorg. Chem.* **31**, 4843–4848 (1992).
22. Chen, J. et al. Tuning the reactivity of mononuclear nonheme manganese(IV)-oxo complexes by triflic acid. *Chem. Sci.* **6**, 3624–3632 (2015).
23. White, M. C., Doyle, A. G. & Jacobsen, E. N. A synthetically useful, self-assembling MMO mimic system for catalytic alkene epoxidation with aqueous H_2O_2. *J. Am. Chem. Soc.* **123**, 7194–7195 (2001).
24. Bigi, M. A., Reed, S. A. & White, M. C. Directed metal (oxo) aliphatic C–H hydroxylations: overriding substrate bias. *J. Am. Chem. Soc.* **134**, 9721–9726 (2012).
25. Miao, C. et al. Proton-promoted and anion-enhanced epoxidation of olefins by hydrogen peroxide in the presence of nonheme manganese catalysts. *J. Am. Chem. Soc.* **138**, 936–943 (2016).
26. Mas-Ballesté, R. & Que, L.Jr. Iron-catalyzed olefin epoxidation in the presence of acetic acid: insights into the nature of the metal-based oxidant. *J. Am. Chem. Soc.* **129**, 15964–15972 (2007).
27. Marson, C. M. New and unusual scaffolds in medicinal chemistry. *Chem. Soc. Rev.* **40**, 5514–5533 (2011).
28. Howell, J. M., Feng, K., Clark, J. R., Trzepkowski, L. J. & White, M. C. Remote oxidation of aliphatic C–H bonds in nitrogen-containing molecules. *J. Am. Chem. Soc.* **137**, 14590–14593 (2015).
29. Osberger, T. J., Rogness, D. C., Kohrt, J. T., Stepan, A. F. & White, M. C. Oxidative diversification of amino acids and peptides by small-molecule iron catalysis. *Nature* **537**, 214–219 (2016).
30. Rennhack, A. et al. Synthesis of a potent photoreactive acidic gamma-secretase modulator for target identification in cells. *Bioorg. Med. Chem.* **20**, 6523–6532 (2012).

31. Obach, R. S. Pharmacologically active drug metabolites: impact on drug discovery and pharmacotherapy. *Pharmacol. Rev.* **65**, 578–640 (2013).
32. Sarabu, R. et al. Discovery of piragliatin—first glucokinase activator studied in type 2 diabetic patients. *J. Med. Chem.* **55**, 7021–7036 (2012).
33. Newman, D. J. & Cragg, G. M. Natural products as sources of new drugs from 1981 to 2014. *J. Nat. Prod.* **79**, 629–661 (2016).
34. D'Accolti, L., Fusco, C., Lampignano, G., Capitelli, F. & Curci, R. Oxidation of natural targets by dioxiranes. Part 6: On the direct regio- and site-selective oxyfunctionalization of estrone and of 5α-androstane steroid derivatives. *Tetrahedron Lett.* **49**, 5614–5617 (2008).
35. Breslow, R., Zhang, X. & Huang, Y. Selective catalytic hydroxylation of a steroid by an artificial cytochrome P-450 enzyme. *J. Am. Chem. Soc.* **119**, 4535–4536 (1997).
36. See, Y. Y., Herrmann, A. T., Aihara, Y. & Baran, P. S. Scalable C–H oxidation with copper: synthesis of polyoxypregnanes. *J. Am. Chem. Soc.* **137**, 13776–13779 (2015).
37. Font, D. et al. Readily accessible bulky iron catalysts exhibiting site selectivity in the oxidation of steroidal substrates. *Angew. Chem. Int. Ed.* **55**, 5776–5779 (2016).
38. Nanjo, T., de Lucca, E. C. Jr & White, M. C. Remote, late-stage oxidation of aliphatic C–H bonds in amide-containing molecules. *J. Am. Chem. Soc.* **139**, 14586–14591 (2017).

Acknowledgements

Financial support for this work was provided by the NIH NIGMS Maximizing Investigators' Research Award MIRA (R35 GM122525). The authors acknowledge The Uehara Memorial Foundation for a fellowship to T.N. and Conselho Nacional de Desenvolvimento Científico e Tecnológico for a fellowship to E.C.L. (proc. no. 234643/2014-5). The authors thank L. Zhu for assistance with NMR spectroscopy, D. Gray and T. Woods for X-ray crystallographic studies, and C. Delaney for preliminary studies on basic nitrogen-containing compounds. The authors also thank C. Wendell, K. Feng and W. Liu for checking the procedures. The data reported in this paper are tabulated in the Supplementary Information.

Author contributions

M.C.W. and J.Z. conceived and designed the project and wrote the manuscript. J.Z., T.N. and E.C.L. conducted the experiments and analysed the data. All authors provided comments on the experiments and manuscript during its preparation.

Competing interests

The University of Illinois has filed a patent application on the Mn(CF_3–PDP) catalyst for methylene oxidation in aromatic molecules.

Additional information

Supplementary information is available for this paper at https://doi.org/10.1038/s41557-018-0175-8.

Reprints and permissions information is available at www.nature.com/reprints.

Correspondence and requests for materials should be addressed to M.C.W.

Publisher's note: Springer Nature remains neutral with regard to jurisdictional claims in published maps and institutional affiliations.